RSC Advances

This is an *Accepted Manuscript*, which has been through the Royal Society of Chemistry peer review process and has been accepted for publication.

Accepted Manuscripts are published online shortly after acceptance, before technical editing, formatting and proof reading. Using this free service, authors can make their results available to the community, in citable form, before we publish the edited article. This *Accepted Manuscript* will be replaced by the edited, formatted and paginated article as soon as this is available.

You can find more information about *Accepted Manuscripts* in the **Information for Authors**.

Table of contents

for

Dual amplifying fluorescence anisotropy for detection of Respiratory syncytial virus DNA fragment with size-control synthesized metal-organic framework MIL-101

Jing Fang Guo,[1] Rong Mei Fang,[3] ChengZhi Huang [1,2] and Yuan Fang Li [1]*

[1] Education Ministry Key Laboratory on Luminescence and Real-Time Analysis, College of

Chemistry and Chemical Engineering Southwest University, Chongqing 400715, P R China;

[2] College of Pharmaceutical Science, Southwest University, Chongqing 400716, China.

[3] Chongqing Three Gorges University, Chongqing 404100, China.

E-mail: liyf@swu.edu.cn Fax: (+86) 23 68367257; Tel: (+86) 23 68254659;

Nano-sized MIL-101 with negligible scattered light synthesized by the additive of glycerol was used to amplify FA for detection of DNA with a dual amplification effect.

ARTICLE TYPE

Dual amplifying fluorescence anisotropy for detection of Respiratory syncytial virus DNA fragment with size-control synthesized metal-organic framework MIL-101
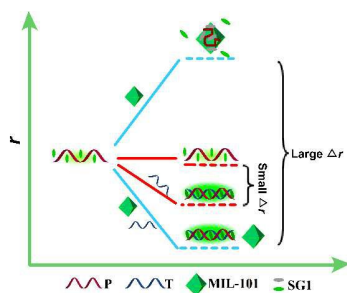
Jing Fang Guo,[1] Rong Mei Fang [3], Cheng Zhi Huang [1, 2] and Yuan Fang Li [1]*

In order to eliminate the scattered light induced by the signal amplifier in fluorescence anisotropy (FA) assay, nanosized metal organic framwork MIL-101, raging from 80nm-500nm, has been synthesized through hydrothermal method with the additive of glycerol. We chose the 100 nm of MIL-101 to enhance
10 FA for lable-free detection of Respiratory syncytial virus (RSV) gene sequence, DNA-intercalating dye SYBR Green I (SGI) as the fluorophore, based on the different affinities of MIL-101 toward ssDNA and dsDNA. The nanosized MIL-101 has negligible scattering effect own to its smaller particle size, so all of the experimental dates of FA values were smaller than the maximum initial anisotropy of 0.4. As a specific advantage, a dual amplification result of not only increased the FA value of SGI/ssDNA (r_1) but
15 also decreased the FA value of SGI/dsDNA (r_2) was presented at the same time. Consequently, a larger FA value change Δr (Δr, $\Delta r = r_1 - r_2$) was obtained and contribute to improve the sensitivity. And the quantitative detection of target DNA (T) was achieved according to the relationship between Δr and the concentration of T. In the presence of MIL-101, the Δr is 7-fold higher than that without MIL-101 and achieved the sensitive and selective detection of RSV DNA.

20 1. Introduction

Fluorescence anisotropy is the measurement for rotational motion-related factors of a fluorophore or fluorophore-labeled complex. In general, molecular volume and mass increases of the fluorophore often lead to a larger FA value.[1] To expand the
25 applications of FA and improve its sensitivity, various materials of large masse including proteins,[2] gold nanoparticle,[3] graphene oxide (GO)[4] and metal-organic framework (MOF)[5] have been employed as mass amplifiers. But, a high anisotropy signal cannot always be obtained by simply enlarging the molecular
30 volume and mass, because this increase may not be able to efficiently retard the rotational movement of the fluorophore.[6] Furthermore, overlarge material is easy to settlement and not suit for analytical use in aqueous solution. Most importantly, an obvious scattered light will be generated for the big size of the
35 amplifier, thus will interfere with anisotropy measurements.[7] Generally, if the measured anisotropy for a randomly oriented sample is bigger than 0.4, one can confidently infer the presence of scattered light in addition to fluorescence.[7-8] There are some reports about nanomaterial used as FA amplification platform for
40 targets assay, yet some of its FA value exceed 0.4, [9] which is unreasonable and not allowed. Furthermore, deduction of scattered light from the measured fluorescence dates often leads demonstrable inaccuracy. So, the application of nanomaterial in enhancing FA needs improvement and standardization. One
45 approach for this problem is to find amplifiers with both appropriate size and excellent amplification ability of FA.

MOFs have achieved remarkable progresses in wide range of applications.[10] Despite the more traditional areas of storage,[11] separation,[12] and catalysis,[13] some interesting MOF structures
50 also exhibited great potential in sensing,[14] molecular recognition,[15] and biological applications.[16] In our previous study, we utilized Chromium-benzenedicarboxylates (MIL-101) as the FA amplification platform for sensitive detection of DNA,[5] which is simple and effective. Yet, an obvious scattered light exists for
55 the large size of MIL-101, thus interfere with the FA measurement. So far, the synthesis of MOF-type materials has been studied extensively.[17] However, the morphology control of MOFs, especially to get nano-sized MOFs, has not been investigated enough even though it is very important because the
60 nanoscale MOFs have potential applications like drug delivery,[18] imaging[19] and other analytical application in aqueous solution. Therefore, it is necessary to pay more attention on the investigation and synthesis of nano-sized MOFs.

Herein, in order to facilitate MOFs to have a better
65 performance in FA assay, nanosized metal organic framework MIL-101, ranging from 80 - 500nm has been synthesized through traditional hydrothermal method[20] with the additive of glycerol. The obtained smaller size MIL-101 posses better monodispersity and weaker scattered light. Furthermore, the zeta potential of the
70 MIL-101 increased with the decreasing of size (Fig. 2, a). So, if this developed MIL-101 performing as the FA amplifier for DNA detection, the electrostatic interaction between MIL-101 and DNA would be strengthened. And the FA amplification effect will still be obvious or even greater than before.

In this contribution, we chose the 100 nm of MIL-101 to amplify FA for lable free detection of Respiratory syncytial virus (RSV) DNA sequence based on its different affinities of MIL-101 toward ssDNA and dsDNA. As show in scheme 1, without MIL-101, only small FA change occurred for the little molecular mass variation before and after the hybridization of (probe DNA) P with T. Conversely, in the presence of ML-101, the FA of SGI/ssDNA sharply increased and the FA value of SGI/dsDNA become smaller than that of SGI/dsDNA without MIL-101. So, a dual FA amplification effect is presented and a larger Δr value is obtained, which is beneficial to FA assay. Furthermore, in the whole experiment, all of the measured FA values are smaller than 0.4, indicating the scattered light of MIL-101 is negligible.
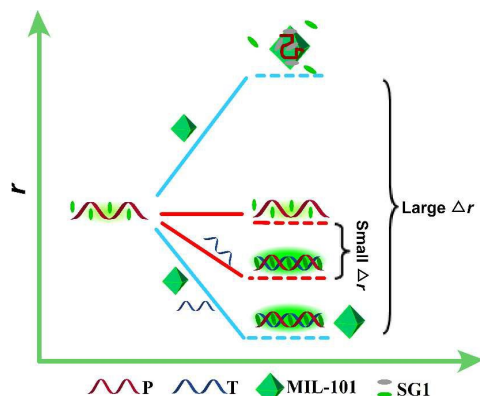
Scheme 1 The concept and the principle of MIL-101 amplified fluorescence anisotropy strategy for lable-free detection of RSV DNA.

2. Experimental section

2.1 Materials

$Cr(NO_3)_3 \cdot 9H_2O$ (99%), hydrofluoric acid (HF) (48%) and terephthalic acid (H_2BDC) (99%) were purchased from Aladdin chemistry Co.Ltd. (Shanghai, China). Herein, we used oligonucleotides of a specific sequence (5′-AAA AAT GGG GCA AAT A-3′) as the probe for recognition of RSV DNA sequence (target DNA). All of the ssDNAs were synthesized and purified by Sangon Biotech Co.Ltd (Shanghai, China), and were used without further purification. The sequence of the complementary target DNA (T) was 5′-TAT TTG CCC CAT TTT T-3′. One-base-mismatched oligomer (MT1), 5′-TAT TTG CCC CAT TTT T-3′; two-base-mismatched oligomer (MT2), 5′-TAT TTG CCC CAT TTT T-3′; three-base-mismatched oligomer (MT3), 5′-TAT TTG CCC CAT TTT T-3′. SG (10000 ×) was purchased from invitrogen inc, which was diluted to 1.25 × with water to make a stock solution. The concentration of 125 × SG is 0.245 mM, according to the research of Liu *et al*. in 2008.[21]

2.2 Apparatus

An S-4800 scanning electron microscope (SEM) (Hitachi, Japan) was used to scan the SEM images. A Model JASCO-810 spectropolarimeter (JASCO, Japan) was employed to measure circular dichroism (CD) spectra. A XD-3 X-ray diffractometer with Cu K_α radiation ($\lambda = 1.5406$ Å) was used to collect powder X-ray diffraction (PXRD) patterns at a scan rate of 2.00 min^{-1} (Purkinje, China). Fluorescence anisotropy was measured with an F-2500 fluorescence spectrophotometer equipped with a polarization filter (Hitachi, Tokyo, Japan). Oakton pH 510 meter

(Singapore) was employed to adjust the pH values. Vortex mixer QL-901 (Haimen, china) was employed to blend the solution. Millipore water from Milli-Q filtration syetem (Millipore, USA) was employed to prepare all the solutions.

2.3 Preparation of MIL-101

Nanosized MIL-101 ranging from 80 - 500 nm was synthesized according to the published procedure with some modifications.[20] Briefly, $Cr(NO_3)_3 \cdot 9H_2O$ (2.00 g, 5.0 mM), HF (48 wt%, 5.0 mM), terephthalic acid (0.82 g, 5.0 mM) and 24 mL of deionized water and a certain amount of glycerol were added into a hydrothermal bomb and then put it in an autoclave held at 220°C for 20 h. After that, the mixture was naturally cooled to room temperature, followed by filtering the mixture with a large pore fritted glass filter to remove the significant amount of recrystallised terephthalic acid. Then, the product of MIL-101 was separated from the solution using a small pore filter and washed with deionized water and ethanol to remove the glycerol. After being soaked in ethanol (95% ethanol with 5% water) at 80°C for 24 h, it was washed with hot ethanol. Further, MIL-101 powder was refluxed for 24 h in 1 M NH_4F aqueous solution and washed with hot water. To obtain a good dispersion condition, we do not dried the product into powder but keeps as solution for further use. Certainly, we dried 10 mL of the reserves solution into powder, knowing that it's concentration is 40 mg/mL. The structure of MIL-101 was shown in Fig. 1.

2.4 Detection of RSV DNA

Briefly, 50 μL of PB buffer (pH 7.2), 100 μL of probe DNA (0.1 μM) and a certain volume of target DNA (0.1 μM) were sequentially added into a 1.5 mL tube, and kept at 30°C for 40 min. Then 50 μL of SG (2.45 μM) was added and incubated at room temperature for 5 min. Last, 35 μL of MIL-101 solution (0.05 mg/mL) was added into the mixture and further diluted with ultrapure water to 500 μL. After 20 min incubation, fluorescence anisotropy measurements were carried out on the F-2500 fluorescence spectrophotometer with an excitation wavelength of 490 nm and emission intensity at 529 nm was recorded. Then the FA value was calculated according to the Perrin equation.[4, 22]

3. Results and discussion

3.1 Charactrization of the synthesised MIL-101 and the effect of the volume of glycerol on the particle size
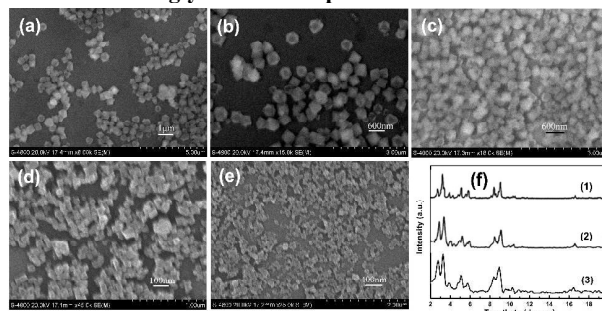

Fig. 1 (a) ~ (e): SEM images of synthesized MIL-101s to show the effect of amount of glycerol on particle size (a ~ e, the volume of glycerol was 0, 30, 50, 80, 100 μL, respectively); (f): Powder X-ray diffraction (XRD) spectra of MIL-101 (a) ~ (e) (Fig.1f, 1-5, respectively) and simulated XRD of MIL-101(Fig.1, f6).

Fig. 1 displays SEM images and XRD of the synthesized MIL-

101s synthesized with the addition of different amount of glycerol. As we can see, the particle size decreased with the increasing amount of glycerol. The particle size of MIL-101 was about 500 nm in the absence of glycerol (a). In the presence of 30 μL glycerol, the particle size has no obvious change compared with that without glycerol (b). With the addition of 50μL, 80μL, 100μL of glycerol, the particle size was about 300 nm, 100 nm and 80 nm (c ~ e), respectively. Besides, synthesized MIL-101 was regular octahedron and all the PXRD of different size of MIL-101 were consistent with that of previously reported literature,[20] suggesting that the glycerol has not participated in coordination.

The decreased size of MIL-101 for the additive of glycerol may be explained with the slowed rate of crystal growth than before.[23] As one of the methods for miniaturization of MOF crystals, some organic additives can regulate the crystal size and morphology.[24] Glycerol has been reported that as the additive for size-control synthesis of zeolite A[25] and silver nanoparticles.[26] Similar to these reports, in our experiments, glycerol may also perform as capping agents to suppress the crystal growth, resulting in a decrease of the crystals size.[24] At the same time, the addition of glycerol increased the monodispersity of MIL-101 own to the hydroxyl groups.
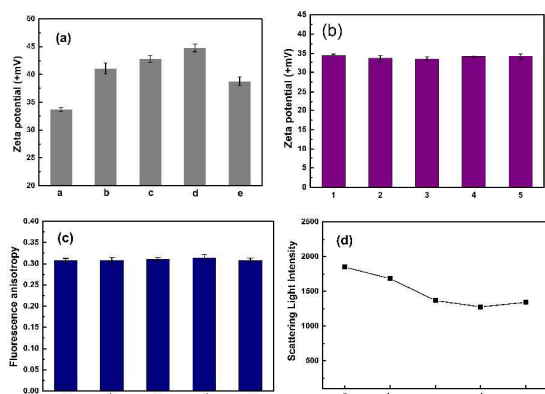

Fig. 2 (a) Zeta potentials of different size MIL-101s synthesized with different amount of glycerol (a~e, 0, 30, 50, 80, 100 μL, respectively). (b) Zeta potential of already synthesized MIL-101 with the addition of different amount of glycerol (1~5, 0, 30, 50, 80, 100 μL, respectively). (c) Similar fluorescence anisotropy value induced by certain amount of different size of MIL-101 and (d) the scatted light intensity they produced, respectively(a~e represent the obtained different size of MIL-101 when of glycerol were 0, 30, 50, 80, 100 μL, respectively). Concentrations: P, 20 nM; SG, 0.245 μM. Tris-HCl buffer, pH 7.2.

As we can see from Fig. 2, the MIL-101 of 100 nm (the addition volume of glycerol was 80 μL) has the largest zeta potential among the different size of MIL-101 (Fig. 2, (a), d). But the zeta potential has no obvious change if we added different amount of glycerol after the MIL-101 synthesized (Fig. 2, (b)). Besides, when the same FA value was induced by different size of MIL-101 (Fig. 2, (c)) the scattering light intensity of 100 nm MIL-101 is the lowest (Fig. 2, (d), d). So, 100 nm of MIL-101 was chosen for further experiments.

3.2 The interaction between SG/DNA complex and MIL-101

As shown in Fig. 3, in the absence of MIL-101, the FA value changed from 0.14 to 0.1 with the small Δr_1 of 0.04 before and after hybridization. However, with the addition of MIL-101, ssDNA can be absorbed on the surface of MIL-101 mainly through electrostatic and π-π stacking interactions.[5] The rotation

of SGI/ssDNA was confined by MIL-101, thus FA value sharply increased to 0.38. And once P was hybridized with T at first, the formed dsDNA of has stable conformation to stay away from MIL-101 and the obtained FA was only about 0.09. So, in the presence of MIL-101 the FA value change (Δr_2) was 0.29, which is 7-fold higher than that of without MIL-101 (Δr_1=0.04). The amplified Δr resulting from the remarkably larger mass change induced by MIL-101, according to the Perrin equation.[22] Specifically, in the presence of MIL-101, the FA of P (r_1) increased and the FA of P+T (r_2) decreased conversely. In another word, herein the MIL-101 played a dual amplification effect of amplifying the FA value of P and reducing the FA value of P/T, thus obtained a larger Δr. This is one of the advantages of employed MIL-101 as amplifier in this lable-free DNA detection strategy compared with other amplification platforms and labled fluorophor.

The reason for the dual amplification phenomenon may be explained as follows. In the presence of MIL-101, FA of ssDNA (r_1) sharply increased for the rotation of ssDNA was significantly confined compare with that without MIL-101. The species of metal ion in the MOF, framework and BET surface of the MOF maybe the factors for MIL-101 to combine with ssDNA. Consequently, the FA valve was amplified. After the addition of target DNA, P hybridized with T, and the positive charged SGI intercalated into the formed dsDNA. So, the electrostatic repulsion between positive charged MIL-101 and SGI interfere the rotation of dsDNA to be faster and more irregular than that without MIL-101, thus lead to a smaller FA value of dsDNA (r_2). As a result, Δr ($\Delta r=r_1-r_2$) was dually amplified. Furthermore, MIL-101 is a 3D Zeotype achitecture, which can adhere the flexible ssDNA but difficult for rigid dsDNA to adsorb. This is beneficial for MIL-101 to distinguish ssDNA and dsDNA. It is expected that further researches can be done to make the mechanism more clearly.
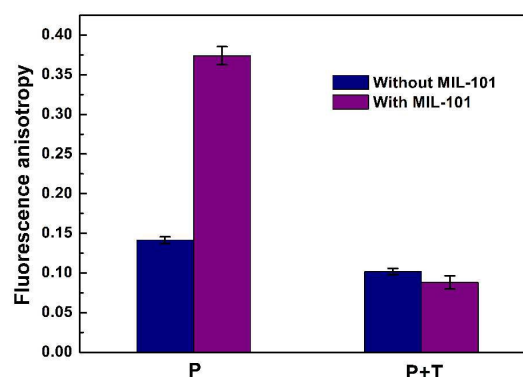

Fig. 3 Fluorescence anisotropy of P and P+T in the absence (navy columns) and presence (purple columns) of MIL-101. Concentrations: P, 20 nM; T, 15 nM; MIL-101, 3.5 μg/mL; pH, 7.2; λ_{ex}, 490 nm.

3.3 Optimization of experimental conditions

Several factors including the dosage of MIL-101, pH value and incubation time were optimized to obtain the best quantitative result. Performing as the amplification platform, the amount of MIL-101 plays a significant role on the target quantification. Insufficient amount of MIL-101 would cause MIL-101 integrate with part of P, resulting in lower background FA value (r_1). However, overdose of MIL-101 would interact with the formed

P/T in some degree and inhibit its releasing, leading to a bigger recovery FA value (r_2). Thus, bring about smaller Δr value ($\Delta r = r_1 - r_2$). Additionally, positively charged MIL-101 can interact with negatively charged DNA through electrostatic interaction. Therefore, pH of the environment would have great influence on FA value. Experimental showed that the optimal conditions were 20 nM of P hybridize with T at 30 °C for 40 min and then incubated with 3.5 µg/mL of MIL-101 (Fig. 4, a) at pH 7.2 for 15 min (Fig. 4, b-c).
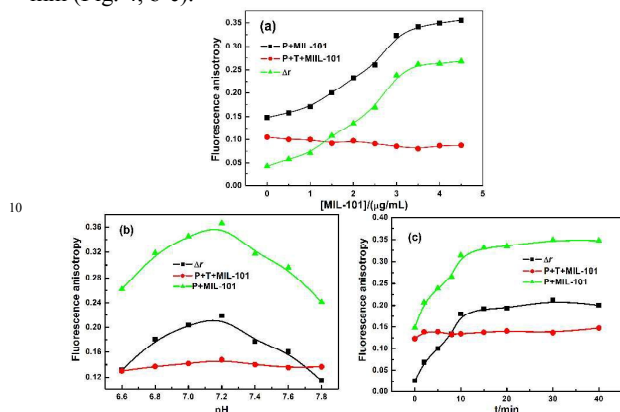

Fig. 4 Fluorescence anisotropy of P (dark line), P+T (red line) and Δr at different concentrations of MIL-101 (a), pH (b) and incubation time (c). Concentrations: P, 20 nM; SG, 0.245 µM, pH 7.2.

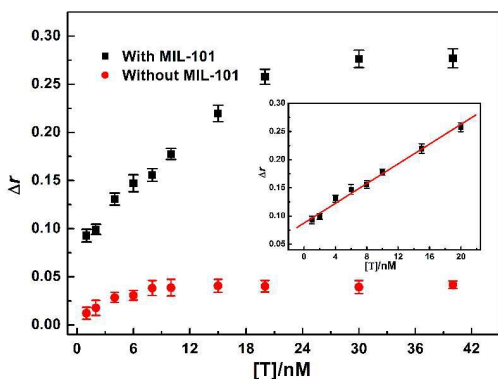### 3.4 High sensitivity and selectivity for RSV DNA detection

Fig. 5 Fluorescence anisotropy changes Δr against the increasing concentration of T from 1 nM to 40 nM with (dark line) and without (red line) the presence of MIL-101. P, 20 nM; MIL-101, 3.5 µg/ml; pH, 7.2; λ_{ex}: 490 nm.

Under the optimal condition, the relationship between the FA value change (Δr) of SGI and the concentration of target DNA is investigated. Fig. 5 shows the dependence of Δr before and after the P, T hybridization on the increasing concentration of T. In the presence of MIL-101, there is a linear relationship between them in the range of 1-20 nM with linear regression equation of $\Delta r = 0.087 + 0.0088\ c_T$ and the detection limit of 1 nM ($S/N = 3$). Contrastively, in the absence of MIL-101, the Δr has no obvious change with the increasing concentration of T. Apparently, MIL-101 can remarkably enhance Δr mainly attribute to its FA amplification effect on SGI/ssDNA. The result confirms that this strategy can be successfully applied for quantitative detection of RSV DNA.

In this study, to evaluate the feasibility and sequence specificity, control experiments were carried out by comparing Δr of target DNA with that of different mismatched target DNA. As shown in Fig. 6, in the presence of MIL-101, the specificity of the assay is excellent. Based on the different hybridization efficiency

of targets with P, the addition of T produces significant Δr increasement, while the mismatched targets M1, M2 and M3 give relatively lower Δr and T can be easily distinguised from M1, M2 and M3. However, in the absence of MIL-101, there is negligible difference among the Δr values of T, M1, M2 and M3 . Besides, all of their value are very small. Therefore, this proposed method using MIL-101 as a FA amplification platform provides high sensitivity and selectivity in RSV DNA detection.
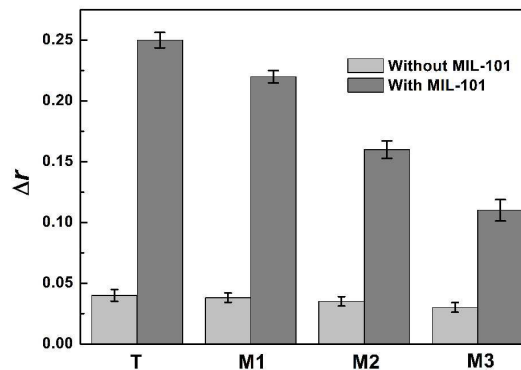

Fig. 6 Specificity of target DNA assay over mismatched DNA in the absence (light gray) and presence (dark gray) of 3.5 µg/ml MIL-101. Concentrations: P, 20 nM; T, M1, M2 and M3 are all 15 nM; pH, 7.2; λ_{ex}: 490 nm.

3.5 Mechanism of the interaction between DNA and MIL-101

Sample name	Zeta potential (mV)
MIL-101	-17.3
MIL-101+P	-27.4
MIL-101+P+T	-23.5
MIL-101+P+SGI	-25.5
MIL-101+P+T+SGI	-21.3

Table 1 Zeta potential variation of MIL-101 in different samples

Electrostatic plays an important role in the interaction between MIL-101 and DNA. Therefore, the zeta potential variation measurement of MIL-101 throughout the reaction process can illustrates the mechanism on the one hand. Table 1 shows the zeta potential variation of different MIL-101 samples. MIL-101 was positively charged with the zeta potential of +33.2 mV in water. To reflect the real situation during the experiments more accurately, we tested the zeta potential of MIL-101 samples under the experimental condition. The measured zeta potential of MIL-101 was -17.3 mV in the presence of pH 7.2 buffer solution. But the variation tendency of different samples can also used for mechanism explanation. After the addition of negatively charged ssDNA, the zeta potential decreased to -27.4 mV, suggesting that the ssDNA twined onto the suface of MIL-101 and neutralized part of its potential. After the addition of target DNA, the formed dsDNA has a more stable conformation to stay away from the surface of MIL-101. So, the zeta potential is larger. In the presence of positively charged SGI, the variation tendency is consistent to that without SGI. So, the measured results is consistent with the mechanism we proposed.

To further demonstrate the proposed mechanism, we measured the circular dichroism (CD) of P and P/T in the presence and absence of MIL-101 (Fig. 7). As is known, dsDNA processes a typical DNA spectrum with the positive and negative peak at 275 nm and 246 nm (crossover point, 258 nm),[27]

respectively. And the measured results are consistent with that reported. Compared with the spectrum of P, an increase in the amplitude of the negative CD band was observed in the prescence of target DNA. So, the DNA helicity increased and the dsDNA structure formed. Futhermore, the peaks' location has not changed in the prescence of MIL-101, suggesting that the introduction of MIL-101 did not damaged the structure of DNA.[28] The results is not only an evidence for the mechanism, but also interpreted the feasibility of MIL-101 for this application.
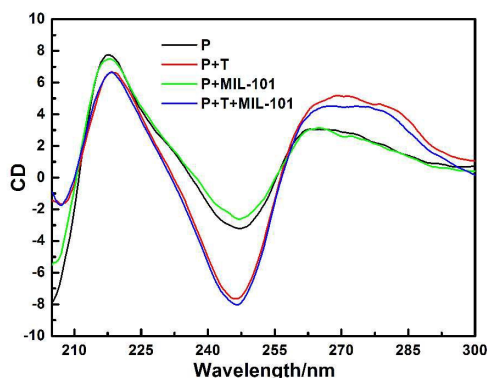

Fig. 7 Circular dichroism of P and P/T in the absence and presence of MIL-101. Concentrations: P, 1.2 µM; T, 1.2 µM; SG, 0.245 µM; MIL-101, 3.5 µg/mL. pH 7.2.

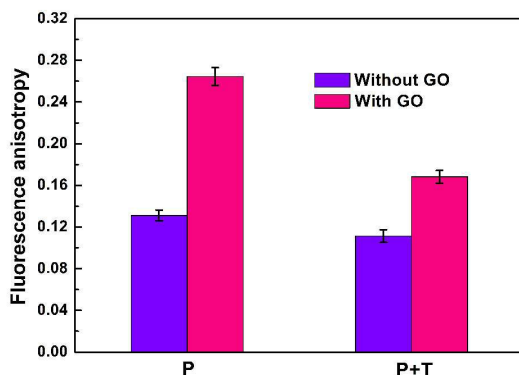### 3.6 Amplification ability comparision between MIL-101 and GO

Fig. 8 Fluorescence anisotropy of P and P/T in the absence (violet columns) and presence (pink columns) of GO.

There are several reports about graphene oxide performed as the fluorescence anisotropy amplication platform for metal ion[29] and other targets detection,[9] which also present good performance. Under the same condition to our experiments, we applied GO to enhance FA for detection RSV DNA fragment. As shown in Fig. 8, in the prescence of GO, both the FA value of P and P/T are enlarged. So, GO did not shown the dual amplication ability, which is inferior to MIL-101. As we mentioned above, it maybe just the special structure and chemical property of MIL-101 facilitate the dual amplification effect.

4. Conclusion

In conclusion, well dispersion of nanosized metal organic framwork MIL-101 ranging from 80nm-500 nm has been synthesized with the organic additive of glycerol. The 100 nm of MIL-101 was successfully used to enhance FA for lable-free detection of RSV DNA with a dual amplification ability. The scattered light produced by the nanosized MIL-101 is negligible,

which guaranteed the measured FA value were smaller than the maximum initial anisotropy of 0.4. The addition of glycerol not only decreased the size of MIL-101 but also increased its monodispersity own to the hydroxyl groups. We expect that this newly synthesized nanosized MIL-101 will find its better uses for analytical application which require MOFs with small size, such as cell imaging and drug delivery. On these basses, it will be more favorable for FA assay if the fluorescence of fluorophore has no change when FA is amplified by the amplifier, on which we will do more work later.

Notes and references

[1]Education Ministry Key Laboratory on Luminescence and Real-Time Analysis, College of Chemistry and Chemical Engineering Southwest University, Chongqing 400715, [2]College of Pharmaceutical Science, Southwest University, Chongqing 400716, China.[3]Chongqing Three Gorges University, Chongqing 404100, China. Fax: (+86) 23 68367257; Tel: (+86) 23 68254659; E-mail: liyf@swu.edu.cn

1. M. E. McCarroll, F. H. Billiot. and I. M. Warner. *J. Am. Chem. Soc.*, 2001, **123**, 3173-3174.

2. J. N. Zhang, J. N. Tian, Y. L. He, Y. C. Zhao and S. L. Zhao, *Chem. Commun.* , 2014, **50**, 2049-2051.

3. B.-C. Ye and B.-C. Yin, *Angew. Chem. Int. Ed.*, 2008, **47**, 8386-8389.

4. Y. Yu, Y. Liu. S. J. Zhen and C. Z. Huang, *Chem. Commun.*, 2013, **49**, 1942-1944.

5. J. F. Guo, C. M. Li, X. L. Hu, C. Z. Huang and Y. F. Li, *RSC Advances*, 2014, **4**, 9379-9382.

6. M. J. Zou, Y. Chen. X. Xu, H. D. Huang, F. Liu and N. Li, *Biosens. Bioelectron.*, 2012, **32**, 148-154.

7. J. R. Lakowicz, *Principles of fluorescence spectroscopy*, Springer press, New York, 3rd edn, 2006, P, 2358.

8. A. N. Bader, E. G. Hofman. Paul M. P. van Bergen en Henegouwen and H. C. Gerritsen, *OPT. EXPRESS*, 2007, **15**, 6934-6945.

9. J. H. Liu, C. Y. Wang, Y. Jiang, Y. P. Hu, J. H. Li, S. Yang, Y. H. Li, R. H. Yang, W. H. Tan and C. Z. Huang, *Anal. Chem.*, 2013, **85**, 1424-1430.

10. Z.-Y. Gu, C.-X. Yang. N. Chang, X.P. Yan, *Acc. Chem. Res.*, 2012, **45**, 734-745.

11. B. Li, H. M. Wen, H. L. Wang, H. Wu, M. Tyagi, T. Yildirim, W. Zhou and B. L. Chen, *J. Am. Chem. Soc.*, 2014, **136**, 6207-6210.

12. (a) W. Y. Wu, A. M. Kirillov, X. H. Yan, P. P. Zhou, W. S. Liu and Y. Tang, *Angew. Chem. Int. Ed.*, 2014, 53, 1-6. (b) Z. Y. Gu and X. P. Yan, *Angew. Chem. Int. Ed.*, 2010, 49, 1477-1480; (c) N. Chang, Z. Y. Gu and X. P. Yan, *J. Am. Chem. Soc.*, 2010, 132, 13645-13647.

13. J. W. Liu, L. F. Chen, H. Cui, J. Y. Zhang, L. Zhang and C. Y. Su, *Chem. Soc. Rev.*, 2014, **43**, 6011-6061.

14. (a) P. L. Feng, K. Leong and M. D. Allendorf, *Dalton Trans.*, 2012, **41**, 8869-8877; (b) B. Liu, W. P. Wu, L. Hou and Y. Y. Wang, *Chem. Commun.*, 2014, **50**, 8731-8734; (c) L. E. Kreno, K. Leong, O. K. Farha, M. Allendorf, R. P. Van Duyne and J. T. Hupp, *Chem. Rev.*, 2012, **112**, 1105-1125.

15. (a) H. W. Li, X. Feng, Y. X. Guo, D. D. Chen, R. Li, X. Q. Ren, X. Jiang, Y. P. Dong and B. Wang, *Sci. Rep.*, 2014, **4**, 4366; (b) B. L. Chen, S. C. Xiang. and G. D. Qian, *Acc. Chem. Res.*, 2010, **43**, 1115-1124.

16. N. J. Hinks, A. C. McKinlay, B. Xiao, P. S. Wheatley and R. E. Morris, *Microporous Mesoporous Mater.*, 2010, **129**, 330-334.

17. (a) T. Kundu, S. C. Sahoo and R. Banerjee, *Chem. Commun.*, 2012, **48**, 4998-5000; (b) N. Y. Zhu, G. Tobin and W. Schmitt, *Chem. Commun.*, 2012, **48**, 3638-3640; (c) N. Stock and S. Biswas, *Chem. Rev.*, 2012, **112**, 933-969.

18. (a) P. Horcajada, C. Serre. G. Maurin, N. A. Ramsahye, F. Balas, M. ValletReg. M. Sebban, F. Taulelle and G. Férey, *J. Am. Chem. Soc.*,

2008, **130**, 6774-6780; (b) K. M. L. Taylor-Pashow, J. D. Rocca. Z. G. Xie, S. Tran and W. B. Lin *J. Am. Chem. Soc.*, 2009, **131**, 14261-14263.

19. K. M. L. Taylor, A. Jin and W. B. Lin, *Angew. Chem. Int. Ed.*, 2008, **120**, 7836-7839.

20. (a) G. Ferey, C. Mellot-Draznieks, C. Serre, F. Millange, J. Dutour, S. Surble and I. Margiolaki, *Science*, 2005, **309**, 2040; (b) H. L. Liu, Y. L. Liu, Y. W. Li, Z. Y. Tang and H. F. Jiang, *J. Phys. Chem. C*, 2010, **114**, 13362-13369.

21. J. Wang and B. Liu, *Chem. Commun.*, 2008, 4759-4761.

22. D. M. Jameson and J. A. Ross, *Chem. Rev.*, 2010, **110**, 2685-2708.

23. N. A. Khan, I. J. Kang, H. Y. Seok and S. H. Jhung, *Chem. Eng. J.*, 2011, **166**, 1152-1157.

24. V. Valtchev and L. Tosheva, *Chem. Rev.*, 2013, **113**, 6734-6760.

25. J. F. Yao, L. Yu, L. X. Zhang and H. T. Wang, *Mater. Lett.*, 2011, **65**, 2304-2306.

26. D. Steinigeweg and S. Schlucker, *Chem. Commun.*, 2012, **48**, 8682-8684.

27. A. J. Patil, J. L. Vickery, T. B. Scott and S. Mann, *Adv. Mater.*, 2009, **21**, 3159-3164.

28. J. M. Fang, F. Leng, X. J. Zhao, X. L. Hu and Y. F. Li, *The Analyst*, 2014, **139**, 801-806.

29. Y. Zhang, Y. Liu, S. J. Zhen and C. Z. Huang, *Chem. Commun.*, 2011, **47**, 11718-11720.